

Density-Functional Theory of Elastically Deformed Finite Metallic System: Work Function and Surface Stress[¶]

V. V. Pogosov^{a,*}, and V. P. Kurbatsky^{ab}

^aDepartment of Microelectronics

^bDepartment of Physics, Zaporozhye State Technical University, Zaporozhye, 69063 Ukraine

*e-mail: vpogosov@zstu.edu.ua

Received August 3, 2000

Abstract—We study the external strain effect on the surface properties of simple metals within the framework of a modified stabilized jellium model. We derive the equations for the stabilization energy of the deformed Wigner–Seitz cells considered as a function of the bulk electron density and the given deformation. The results for the surface stress and the work function of aluminium calculated using the self-consistent Kohn–Sham method are also given. The problem of anisotropy of the work function of a finite system is discussed. A clear explanation of independent experiments on the stress-induced contact potential difference at metal surfaces is presented. © 2001 MAIK “Nauka/Interperiodica”.

1. INTRODUCTION

The early experimental investigations of the force acting on electrons and positrons inside a metal tube in the gravitational field of the Earth [1, 2] raised a question about the influence of metal deformation on the electron work function. The direct measurements using the Kelvin method showed a decrease/increase of the contact potential difference (CPD) of the stretched/compressed metal samples [3–5]. Similarly, the experiment with a high-speed spinning metal rotor nonuniformly deformed over the length demonstrated that the CPD changes between areas of the surface subjected to different deformations [6] (see also the discussion of the earlier experiments by Harrison [7]). The influence of the deformation on the electron emission from a thin metal film has also been investigated [8]. Recently, a similar effect on the CPD was observed at the surface of a sample with a nonuniform distribution of the residual mechanical stress [9]. These at first sight surprising results imply the respective increase/decrease of the work function with the uniaxial tension/compression of the metal sample. All these experiments raise two important questions that must be answered by the microscopic theory: (i) Does the change of the CPD correspond to a change in the work function? (ii) What is the sign of the deformation gradient of the surface energy and the work function for a metal subject to the tension (or compression) along some direction?

The first question is related to violation of the local electroneutrality of the metal and hence, to non-equipotentiality of its geometric surface. The second question stems from the general statement of the elasticity theory: the change in the total energy of a solid is propor-

tional to the square of the relative deformation. Therefore, the energy must increase for compression as it does for tension. On the other hand, it was found experimentally that, in the elastic deformation range, a uniaxial deformation of a metal sample leads to a linear change in the CPD [4, 5]. This implies that the classical elasticity theory is not completely correct in determining elastic characteristics of surfaces. This question is also important in determining the surface tension or the surface stress for macroscopic samples [10] and small metal particles [11].

The measurements of the derivative of surface tension of a solid with respect to the electrical variable (the so-called “estans” [12]) indirectly show a small difference between the surface stress and the surface energy. On the other hand, different calculations [13–15], including the ones based on the first principles [16], show an appreciable difference between these two quantities. A rough estimation of the difference between the surface energy and the surface stress can also be done using the cohesive energy and the vacancy formation energy. In the continuum approximation, the cohesive energy (or the atomic “work function”) ϵ_{coh} and the vacancy formation energy ϵ_{vac} give respectively the irreversible and reversible work required for the creation of a new spherical surface of the Wigner–Seitz cell with the radius r_0 . Following [17], we have

$$\epsilon_{coh} \approx 4\pi r_0^2 \gamma_0 (1 + \delta/r_0),$$

where γ_0 is the surface energy per unit area of the flat surface and δ is the size correction for the surface of a positive curvature.

[¶]This article was submitted by the authors in English.

The reversible work for the creation of a vacancy (which can be defined as the work needed for blowing a small bubble) is given by [18] δ/r_0

$$\varepsilon_{vac} \approx \int_0^{r_0} dr 4\pi r^2 [2\tau_0(1 - \delta/r)/r] = 4\pi r_0^2 \tau_0 (1 - \delta/r_0).$$

where we introduce a well-defined physical quantity—the surface stress of the flat surface τ_0 —to describe a tensed curved surface [19, 20]. Combining the expressions for ε_{coh} and ε_{vac} , we obtain

$$\tau_0 \approx \gamma_0 \left(\frac{1 + \delta/r_0}{1 - \delta/r_0} \right) \frac{\varepsilon_{vac}}{\varepsilon_{coh}}.$$

The Kohn–Sham calculations in [21, 22] give $\delta/r_0 \approx 0.40$ and 0.52 for Na and Al, and the ratio of the experimental values $\varepsilon_{vac}/\varepsilon_{coh}$ is approximately equal to $1/2$ and $1/3$, respectively. These values agree very well with $\delta/r_0 \approx 1/2$ obtained in [18], which follows from the Langmuir semiempirical rule [23]. From this simple estimation, it follows that τ_0 is approximately equal to or less than γ_0 .

In this work, we investigate theoretically the surface energy, stress, and work function of an elastically deformed metal. A uniaxial strain applied to the surface introduces anisotropy to the metal by changing the density (or separation) of the atomic planes and the electron gas concentration and contributes to an extra surface dipole barrier. A rigorous study of this problem from first principles is tedious and requires cumbersome numerical computations. On the other hand, the calculations based on the isotropic models of metal, i.e., on the jellium model [24] (which ignores the discrete nature of ions) or the stabilized jellium model (in which interparticle interactions are averaged over volumes of the spherical Wigner–Seitz cells), do not allow one to properly account for the inhomogeneous strain effects.

We develop a modification of the stabilized jellium model in order to describe the metal deformed by the strain [27]. In this modification, the metal energy is expressed as a function of the density parameter r_s and the given deformation. In Section 2, we give a general discussion of the effect of the deformation-induced anisotropy on the work function, which is one of the most important electron surface characteristics. In Section 3, we present equations for the stabilized jellium model accounting for the elastic deformation. In Section 4, the modified stabilized-jellium model is applied to calculate, by the Kohn–Sham method, the effect of the uniaxial strain on the electron surface characteristics of single-crystal aluminum.

2. THE DESCRIPTION OF DEFORMATION

It is important to note that in all experiments we deal with finite samples. Different reticular electron densi-

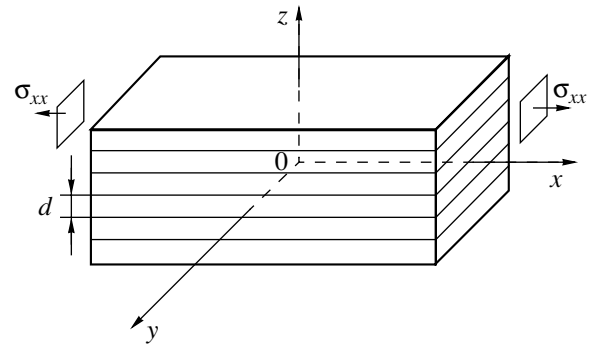


Fig. 1. A qualitative sketch of the sample deformation.

ties at particular faces of a single crystal (crystallite) of an irregular shape lead to different electrostatic potentials for these faces. A similar situation can occur in the deformed metal.

We consider a hypothetical crystal having the shape of a rectangular parallelepiped (see figure). We assume the equivalence of all crystal faces in the undeformed state. This picture breaks down upon the crystal deformation. The four side faces remain equivalent to each other, but not to the two base faces. The electroneutrality condition for the metal sample that is stretched or compressed along the x -axis can be written as

$$\int dx \int dy \int dz [n(x, y, z) - \rho(x, y, z)] = 0, \quad (1)$$

where the electron charge density distribution $n(\mathbf{r})$ attains the magnitude n_0 in the metal bulk. The ion charge distribution can be modeled by the step function,

$$\rho(\mathbf{r}) = \bar{\rho} \theta(\mathbf{r} - \mathbf{r}'),$$

where \mathbf{r}' is the radius vector of the surface, $\bar{\rho} = \bar{n}_0/Z$, and Z is the valence. We use atomic units ($e = m = \hbar = 1$) throughout.

By definition [14], with the electrostatic potential set equal to zero in the vacuum, the electron work function for a face of the semi-infinite crystal is

$$W_{face} = \bar{\phi}_0 - \frac{d}{dn} (\bar{n}_0 \varepsilon_J) - \langle \delta v \rangle_{face}, \quad (2)$$

where $\bar{\phi}_0 < 0$ denotes the electrostatic potential in the metal bulk and $\varepsilon_J \equiv \varepsilon_J(\bar{n}_0)$ is the average energy per electron in the uniform electron gas. The last term represents the difference $\delta v(\mathbf{r})$ between the pseudopotential of the lattice of ions and the electrostatic potential of the positive background averaged over the Wigner–Seitz cell; this term allows us to distinguish between different faces of the crystal (cf. Section 3).

For a deformed sample, we assume that the y - and z -directions are equivalent. The deformation along the x -axis induces an artificial homogeneous anisotropy.

The work functions along the x - and z -directions seem to be different for a finite sample, but this conclusion is not correct. This notion is related to the widely spread point of view (see [28] and references therein) that the work function “anisotropy” is determined by the reticular electron density of a given crystal face. However, the electron work function is defined as the difference between the electron energy level in vacuum and at the Fermi surface. This difference is independent of space directions and coordinates and is constant for a metal sample. The work function (or the ionization potential) is a scalar quantity.

From the standpoint of a finite-size sample, the considerations presented by Smoluchowski [28] and by Lang and Kohn [29] are correct in the case where all faces of the finite sample possess the same atomic packing density. For the cubic crystals, it is a parallelepiped with all its sides having equivalent Miller indices. For a sample of an arbitrary form, the work function in the general case depends on the orientation of all parts of the surface.¹

We note that the “spurious” difference $W_x - W_y$ of the work functions along the x - and z -directions defined using the standard form (2) vanishes. This leads to an important inequality

$$\bar{\phi}_x - \bar{\phi}_z = -\langle \delta v \rangle_x + \langle \delta v \rangle_z \neq 0 \quad (3)$$

that means that the values $\bar{\phi}_x$ and $\bar{\phi}_z$ of the electrostatic potential in the bulk of the metal can be treated as if they corresponded to different semi-infinite crystals. This inequality does not allow us to unambiguously define the work function of a finite macroscopic sample because the surface electrostatic barrier is different for different directions.

To simplify the analysis, we express the electron profile of the sample as

$$n(\mathbf{r}) = n_0(\mathbf{r}) + \delta n(\mathbf{r}) \quad (4)$$

and

$$\bar{\phi} = \bar{\phi}_0 + \delta \bar{\phi}, \quad (5)$$

where $n_0(\mathbf{r})$ and $\bar{\phi}_0$ are the values corresponding to a semi-infinite metal. The “surplus” density $\delta n(\mathbf{r})$ originates from the electron transfer from one crystal side to another [31] and differs from zero only in the near-surface layer. Condition (1) along each direction then takes the trivial form

$$A_i \int_{-\infty}^{\infty} dx [n_0(\mathbf{r}) - \rho(\mathbf{r})] = 0, \quad (6)$$

where $A_i \equiv A_x, A_y, A_z$ are the areas of faces of a macroscopic sample and $A_y = A_z$.

¹ In the special case of a nonzero quadrupole moment of the charge distribution in the elementary cell, the effective potential in the bulk depends on the shape of the sample [30].

Taking Eq. (4) into account, Eq. (6) can be written in the “cross-directional” form

$$A_x \int_{-\infty}^{\infty} dx \delta n(\mathbf{r}) + 2A_y \int_{-\infty}^{\infty} dy \delta n(\mathbf{r}) + 2A_z \int_{-\infty}^{\infty} dz \delta n(\mathbf{r}) = 0, \quad (7)$$

where the surplus charge at each side is proportional to its area. Here, for simplicity of illustration, we assume that $\delta n(\mathbf{r})$ is constant on each side of the sample. It follows from Eq. (7) that

$$\frac{\int_{-\infty}^{\infty} dz \delta n(\mathbf{r})}{\int_{-\infty}^{\infty} dx \delta n(\mathbf{r})} = \frac{A_x}{2A_z}, \quad (8)$$

which means that the charges on these sides have the opposite signs. The entire sample must be neutral.²

The corresponding changes of the electrostatic potential are determined by the Poisson equation, which yields relations for the x - and z -components. These relations have the same form

$$\delta \bar{\phi}_x = -4\pi \int_{-\infty}^{\infty} dx x \delta n(\mathbf{r}) = -C_x x_0, \quad (9)$$

where x_0 and accordingly z_0 are the positions of self-induced charge density at the lateral and base sides and C_x and C_z are constants. This allows us to speak about the appearance of an additional, three-dimensional surface dipole barrier. Since (see Eq. (8))

$$A_x \ll A_z, A_y \quad (10)$$

we have

$$|C_x/C_z| \propto A_z/A_x$$

for the weight coefficients and

$$|\delta \bar{\phi}_y| = |\delta \bar{\phi}_z| \ll |\delta \bar{\phi}_x|$$

for the additional potentials. Using (5), we can rewrite Eq. (3) as

$$\delta \bar{\phi}_x \approx \langle \delta v \rangle_z - \langle \delta v \rangle_x \quad \text{and} \quad \delta \bar{\phi}_z = \delta \bar{\phi}_y \approx 0. \quad (11)$$

Condition (10) means that the work function is weakly dependent on the electron transfer between the faces perpendicular to y - and z -directions, and the mea-

² We note that the phase shift η_k of the single-particle wave function along each direction depends on the potential shape in the vicinity of the surface and the Sugiyama–Langreth neutrality sum rule [32] must be rewritten with the anisotropy (i.e., the self-charging) taken into account [33].

surement of the work function at these faces can therefore be replaced by the measurement for a semi-infinite metal. The true work function can be measured by the Kelvin method in the areas near the edges. These areas correspond to sign changes of the density, $\delta n(\mathbf{r} \approx 0)$. For the photoemission method of measuring the work function, conditions (10) and (11) imply that the registration of electrons must be performed at distances much greater than the linear dimensions of the sample. Otherwise, if the photon energy is not sufficiently high, an electron escaping from the metal does not reach the "infinity" but may transit from one face into the other.

The surplus charge Q_x transferred from one face to the other (see Eq. (9)) can be roughly estimated with the help of the standard electrostatic relation

$$\delta\bar{\phi}_x \approx Q_x / \sqrt{A_x}.$$

Taking into account that

$$A_x \approx N_x 2\pi r_0^2,$$

where N_x is the number of the surface Wigner–Seitz cells of the radius r_0 , we obtain

$$Q_x \approx 3r_0 \sqrt{N_x} \delta\bar{\phi}_x.$$

The condition $Q_x > 0$ means that Q_x electrons are transferred from the base faces to the lateral ones. The surface energy per unit area therefore changes by $-W_x Q_x / A_x$ and $+W_z Q_x / 2A_z$ at the base and the lateral sides, respectively. The ratio of these values corresponds to (7). Here, $W_x Q_x$ is equal to the work needed to remove Q_x electrons from the base side of the metal sample to infinity and W_i is the work function of a given side i . Self-charging of the surface can therefore affect the surface energy anisotropy of the single crystal. For example, for an aluminum sample with $\delta\bar{\phi}_z \approx 0.5$ eV and $N_x = 10^2, 10^4$, the respective electronic charges are $Q_x \approx 1, 10$. It is worth noting that this charge can be very significant for a small crystal (cluster) [34]. Therefore, the elasticity and self-charging effects can play an important role in explaining the recently observed force and conductance fluctuations in stretched metal nanowires [35, 36].

On the ground of the above discussion, and owing to Eq. (11), the properties of a large surface plane of a deformed metal crystal can be calculated in the standard manner.

3. THE MODEL OF A UNIFORMLY DEFORMED METAL

The dependence of the CPD on the uniaxial deformation u_{xx} was measured for polycrystalline stretched samples [4, 5]. We assume that the deformation is a measured quantity and the polycrystal is considered as being assembled of a number of simple crystallites. Qualitatively, the problem can therefore be reduced to

the consideration of tension or compression applied to a single crystal.

We first express the average electron density in the metal as a function of the deformation. For this purpose, we consider an undeformed cubic cell of the side length a_0 and the volume

$$\Omega_0 = a_0^3 = \frac{4}{3}\pi r_0^3, \quad (12)$$

where $r_0 = Z^{1/3} r_s$ is the radius of the spherical Wigner–Seitz cell. For a uniaxially deformed cell elongated or compressed along the x -axis, we can write

$$\Omega = a_x a_y^2 = \frac{4}{3}\pi a b^2, \quad (13)$$

where a_x and $a_y = a_z$ are the sides of the elementary parallelogram and a and b are the half-axes of the equivalent prolate or oblate spheroid of revolution around the x -axis. We also have

$$a_x = a_0(1 + u_{xx}) \quad (14)$$

$$\text{and } a_z = a_0(1 + u_{zz}) = a_0(1 - \nu u_{xx}),$$

where ν is the Poisson coefficient for the polycrystal, and

$$\Omega/\Omega_0 - 1 = u_{xx} + u_{yy} + u_{zz}.$$

It follows from Eqs. (12)–(14) that

$$a = r_0(1 + u_{xx}) \quad \text{and} \quad b = r_0(1 - \nu u_{xx}). \quad (15)$$

Similarly, the spacing between the lattice planes perpendicular to the y - or z -direction is

$$d_u = d_0(1 - \nu u_{xx}), \quad (16)$$

where d_0 is the interplanar spacing in the undeformed crystal. It then follows from (12)–(15) that the average electron density in the deformed metal is given by

$$\bar{n} = \bar{n}_0 \Omega_0 / \Omega = \bar{n}_0 [1 - (1 - 2\nu)u_{xx}] O(u_{xx}^2) \quad (17)$$

and the corresponding density parameter is

$$r_{su} = r_s [1 + (1 - 2\nu)u_{xx}]^{1/3}. \quad (18)$$

Proceeding similarly to the derivation of the equations for the original stabilized jellium model [25], we consider a metal assembled from Wigner–Seitz cells. The average energy per valence electron in the bulk is

$$\varepsilon = \varepsilon_J(\bar{n}) + \varepsilon_M + \bar{w}_R, \quad (19)$$

where the first term gives the jellium energy

$$\varepsilon_J(\bar{n}) = \frac{3k_F^2(\bar{n})}{10} - \frac{3}{4\pi} k_F(\bar{n}) + \varepsilon_{cor}(\bar{n}) \quad (20)$$

consisting of the average kinetic and exchange-correlation energy per electron,

$$k_F = (3\pi^2 \bar{n})^{1/3}.$$

The remaining two terms in (19) represent the average of the repulsive part of the Ashcroft model potential, the Madelung energy. A small band-structure energy term [25, 37] in (19) is neglected.

By transforming the ordinary jellium into the stabilized one, the Coulomb interactions were averaged over the Wigner–Seitz cells, as is usual for an isotropic medium. The uniaxial strain applied to the crystal deforms the spherical Wigner–Seitz cells into ellipsoidal ones. This affects the Madelung energy ε_M that now must be averaged over the volume of the deformed cell. This energy can be expressed similarly to the gravitational energy of the uniform spheroid [38] as

$$\begin{aligned} \varepsilon_M(\bar{n}) &= \frac{1}{Z} \int_{\text{spheroid}} d\Omega \bar{n} \left[-\frac{Z}{r} \right] + \frac{1}{2Z} \int_{\text{spheroid}} d\Omega \bar{n} V(r) \\ &= \begin{cases} -\frac{9Z}{10a} \frac{1}{2p} \log \frac{1+p}{1-p}, & a > b, \\ -\frac{9Z}{10a} \frac{1}{p} \arctan p, & b > a, \end{cases} \end{aligned} \quad (21)$$

where $V(r)$ is the electrostatic potential inside the uniformly charged spheroid, $p = \sqrt{|1 - b^2/a^2|}$ determines the spheroid eccentricity, and the upper/lower case corresponds to a prolate/oblate spheroid, respectively. This expression has the correct limit

$$\varepsilon_M(\bar{n}) \longrightarrow 0.9Z/r_0 \text{ as } u_{xx} \longrightarrow 0.$$

We assume that the shape of ionic cores is not influenced by the deformation and remains spherical; therefore,

$$\bar{w}_R = 2\pi\bar{n}r_c^2.$$

For the potential difference $\delta v(\mathbf{r})$ averaged over the Wigner–Seitz cell [25], we have the same relationship as that for the undisturbed crystal:

$$\langle \delta v \rangle_{WS} = \tilde{\varepsilon} + \varepsilon_M + \bar{w}_R, \quad (22)$$

where the electrostatic self-energy of the uniform negative background inside the spheroid is

$$\tilde{\varepsilon} = -\frac{2}{3}\varepsilon_M. \quad (23)$$

The pseudopotential core radius can be found from the mechanical equilibrium condition depending on the mechanical stress induced in the volume of the cell. To determine the core radius r_c , we note that, for the strained metal, the intrinsic pressure $P = -dE/d\Omega = \bar{n}^2 d\varepsilon/d\bar{n}$ in the bulk of a metal sample is compensated by the pressure exerted by external forces,

$$P = -(\sigma_{xx} + \sigma_{yy} + \sigma_{zz}) = -Y u_{xx} (1 - 2\nu), \quad (24)$$

where σ_{ii} are the mechanical stress tensor components and Y is the Young modulus.

For a strained metal, the averaged energy per electron in the bulk is therefore given by

$$\varepsilon = \varepsilon_J(\bar{n}) + \varepsilon_M + \bar{w}_R + P/\bar{n}. \quad (25)$$

For the ideal metal, $\nu = 1/2$ and $P = 0$. This means that the external force changes not the volume but the shape of a cell or a sample. In the linear approximation, the Madelung energy (21) is well approximated by

$$\varepsilon_M(\bar{n}) \longrightarrow -0.9Z\pi r_{0u}.$$

Inserting the explicit expressions for (20), (21), and (24) in (25), we have from the minimum condition that

$$\begin{aligned} r_c &= \left\{ -\frac{2}{15} \left(\frac{9\pi}{4} \right)^{2/3} r_s + \frac{1}{6\pi} \left(\frac{9\pi}{4} \right)^{1/3} r_s^2 \right. \\ &\quad \left. + \frac{1}{5} Z^{2/3} r_s^2 + \frac{2}{9} r_s^4 \frac{d\varepsilon_{cor}}{dr_s} + \frac{8}{9} \pi r_s^6 P \right\}^{1/2} \Big|_{r_s=r_{su}}. \end{aligned} \quad (26)$$

where r_{su} is the equilibrium density parameter of the strained metal. Here, we assume that the volume of the spheroid is equal to the volume of the equivalent sphere of the radius $r_{0u} = Z^{1/3} r_{su}$.

Taking into account that

$$\langle \delta v \rangle_{WS} = \bar{n} \frac{d}{d\bar{n}} (\varepsilon_M + \bar{w}_R), \quad (27)$$

we obtain for the strained metal at with equilibrium density

$$\langle \delta v \rangle_{WS} = -\bar{n} \frac{d}{d\bar{n}} \left[\varepsilon_J(\bar{n}) + \frac{P}{\bar{n}} \right]. \quad (28)$$

Subsequently, similarly to Perdew *et al.* [25], we can introduce the face dependence of the stabilization potential as

$$\langle \delta v \rangle_{face} = \langle \delta v \rangle_{WS} - \left(\frac{\varepsilon_M}{3} + \frac{\pi\bar{n}}{6} d_u^2 \right). \quad (29)$$

The total energy of a finite crystal can be written as the sum of the bulk E^b and the surface energy E^s , where

$$E^s = \gamma_y 4A_y + \gamma_x 2A_x, \quad (30)$$

with γ_y and γ_x being the respective surface energies per unit area of the lateral and base sides. In the undeformed state, where $\gamma_x = \gamma_y = \gamma_z \equiv \gamma$, surface energy (30) changes by

$$\begin{aligned} dE^s &= 4A_y \left(\gamma \delta_{\alpha\beta} + \frac{d\gamma}{du_{\alpha\beta}} \right) du_{\alpha\beta} \\ &\quad + 2A_x \left(\gamma \delta_{\alpha\beta} + \frac{d\gamma}{du_{\alpha\beta}} \right) du_{\alpha\beta}, \end{aligned} \quad (31)$$

Table 1. The calculated surface energies γ , the work function W , the strain derivative $d\gamma/du_{xx}$, and the surface stress τ_{xx} , for elastically deformed Al ($r_s = 2.06$) samples

| Metal | Face | γ , erg/cm ² | W , eV | u_{xx} | $d\gamma/du_{xx}$, erg/cm ² | τ , erg/cm ² | ΔW , eV |
|-------|-------|--------------------------------|----------|----------|---|------------------------------|-----------------|
| Al | (111) | 946 | 4.096 | (+) | 460 | 1406 | -0.032 |
| | | | | (-) | 400 | 1346 | +0.033 |
| | (100) | 1097 | 3.780 | (+) | 833 | 1930 | -0.025 |
| | | | | (-) | 810 | 1907 | +0.016 |

Note: $u_{xx} = \pm 0.03$, positive and negative deformations are labeled with (+) or (-). ΔW is the work function difference. The value of Young's modulus for Al is 70 GPa [39].

where α and β denote directions in the plane of the lateral and base sides and $\delta_{\alpha\beta}$ is the Kronecker symbol. In our model, we calculate only

$$\tau_{xx} = \gamma + \frac{d\gamma}{du_{xx}}. \quad (32)$$

The work function is calculated using the displaced-profile-change-in-self-consistent-field (DP Δ SCF) expression instead of Eq. (2).

To discuss our results, it is useful to rewrite Eq. (2) as

$$W_{face} = -v_{eff} - \epsilon_F, \quad (33)$$

where

$$\bar{v}_{eff} = \bar{\phi} + \bar{v}_{xc} + \langle \delta v \rangle_{face}$$

is the effective potential in the bulk giving the total barrier height at the metal–vacuum interface and \bar{v}_{xc} is the exchange–correlation potential in the bulk ($\bar{v}_{xc} = v_{xc}(-\infty)$).

4. RESULTS AND DISCUSSION

To verify the theory presented in Section 3, we solved the Kohn–Sham equations for two most densely packed surfaces of Al represented by the stabilized jellium model. In terms of our model, we consider two regular single crystals of Al such that all their sides are equivalent in the undeformed state. Under the crystal deformation, the four side faces remain equivalent to each other, but not to the two base faces (see figure). The $\langle \delta v \rangle_{face}$ term included into the effective potential allows us to generate the face-dependent density profiles used in calculating the surface characteristics: work function, surface energy, and surface stress. All calculations were carried out for the upper side of the sample (see figure) assuming the polycrystalline value of the Poisson coefficient $\nu = 0.36$ for elastic properties of Al [39].

Within the applied range of deformations $-0.03 \leq u_{xx} \leq +0.03$, the changes in surface quantities remain linear. The positive/negative deformation u_{xx} implies the tension/compression of the side of the sample, i.e., the decrease/increase of the atomic packing density at this side, and the decrease/increase of the mean elec-

tron concentration \bar{n} and the interplanar spacing in the direction perpendicular to the chosen crystal side. For better understanding the crystal effects, we have also performed calculations for the special case of the “ideal” metal with $\nu = 1/2$. In this case, the deformation does not change \bar{n} , however, the second term (the corrugation dipole barrier) in the face-dependent potential (29) is changed.

The results of calculations are summarized in Table 1. As can be seen, the surface energy increases linearly with the applied positive deformation u_{xx} and decreases with the negative one. This means that $d\gamma/du_{xx}$ is positive for either $u_{xx} > 0$ or $u_{xx} < 0$. Accordingly, Eq. (32) gives the values of the surface stress component τ_{xx} , larger than the surface energy. For $u_{xx} > 0$, the surface stress is somewhat larger than for $u_{xx} < 0$. We now consider the “ideal” metal with $\nu = 1/2$. It seems that the ideal metal fits better to the classical definition of the surface stress [19, 20]. This is related to the fact that in the ideal metal subjected to deformation, only the surface area is changed, while the electron concentration in the bulk remains unchanged.

Calculations performed for the Al (111) surface yield the respective strain derivatives $d\gamma/du_{xx} = 247$ and 213 erg/cm² for $u_{xx} > 0$ and $u_{xx} < 0$. These values are much smaller than the ones reported in Table 1. In this case (with $\nu = 1/2$), we can also evaluate the other components of the surface stress as

$$\tau_{zz} = \tau_{yy} = \gamma + d\gamma/du_{yy}.$$

Inserting

$$du_{zz} = du_{yy} = -\nu du_{xx},$$

we obtain

$$\tau_{zz} = \tau_{yy} = \gamma - 2d\gamma/du_{xx} < \gamma.$$

We can make two observations at this point. First, the latter result agrees with our estimation ($\tau < \gamma$) in Section 1 and with the results derived on the basis of the elasticity theory [40], where the τ/γ ratio expressed in terms of the Poisson coefficient ν is given by $(3\nu - 1)/(1 - \nu)$. For $\nu = 1/2$, this formula gives $\tau/\gamma = 1$ and $\nu < 1/2$ for $\tau/\gamma < 1/2$. Second, in order to calculate τ_{zz} and τ_{yy} for a sample stretched along the x -axis, we must use $d\gamma/du_{xx}$

Table 2. The calculated change in the effective potential for elastically deformed surfaces of Al single crystal

| Metal | Face | u_{xx} | $\Delta v_{\text{eff}}, \text{eV}$ |
|-------|-------|----------|------------------------------------|
| Al | (111) | (+) | -0.103 |
| | | (-) | +0.106 |
| | (100) | (+) | -0.064 |
| | | (-) | +0.069 |

for $u_{xx} < 0$, whereas for a compressed sample, we use the corresponding value for $u_{xx} > 0$. This is because the tension applied along the x -direction leads to compressing the sample along the orthogonal (y and z) axes. The calculated surface stress for Al(111) is in a very good agreement with the values resulting from the available *ab initio* calculations: 1441 erg/cm² in [15], and 1249 erg/cm² in [41]. This also improves the results obtained for the ordinary jellium [24, 41] and the previous direct application of the stabilized-jellium model [13].

The work function decreases linearly with u_{xx} , but the relative change is less than 1% (see Table 1) for the considered strains. A similar behavior is observed for $\nu = 1/2$. The dominating component leading to a decrease of W with u_{xx} is a change in the $\langle \delta v \rangle_{\text{face}}$ term. Thus, the change of the work function under the deformation conditions is determined by the competition of negative changes in the exchange-correlation (v_{xc}) and the electrostatic (ϕ_s) components of the effective potential v_{eff} and the positive change in the face-dependent component $\langle \delta v \rangle_{\text{face}}$. A dominant role is played by the change of $\langle \delta v \rangle_{\text{face}}$, while the change in the Fermi energy is negligibly small. An overall decrease/increase of the work function W is determined by a positive/negative shift of the electrostatic potential in the metal interior.

The calculated change of the work function with strain seems to contradict the experimental results [3–6] where the work function was found to increase/decrease with the elongation/compression of the sample. This conclusion was based on the analysis of the measured CPD [3–7, 9, 27]. In what follows, we demonstrate that this contradiction is spurious. The point is that the measurement by the Kelvin method fixes the change of the surface potential. The experimental observations can therefore be explained not as the change of the work function but as the change of the effective potential v_{eff} upon deformation. The Kelvin method gives the value of the potential difference at the surface of a sample, which can be defined as the position of the image plane $z = z_0$ [26]. In distinction to the work function, to which $\langle \delta v \rangle_{\text{face}}$ contributes directly (Eq. (2)), at the image-plane position located outside the geometric surface, the effective potential feels the change in $\langle \delta v \rangle_{\text{face}}$ by means of the self-consistent procedure for solving the Kohn–Sham equations (even though $\langle \delta v \rangle_{\text{face}}$ is nonzero inside the sample only). The

calculations performed for Al(111) demonstrate that the ratio of the effective potential differences Δv_{eff} of the strained ($u_{xx} = \pm 0.03$) and strain-free samples at the surface and in the bulk is

$$\Delta v_{\text{eff}}(z = z_0) / \Delta \bar{v}_{\text{eff}} \approx 0.8.$$

Here, v_{eff} denotes the respective difference in the metal bulk.

The results for $\Delta v_{\text{eff}}(z_0 : u_{xx})$ are shown in Table 2. The potential difference outside the sample is more negative as the deformation increases. The calculated changes in the effective potential have the same sign as the CPD measured for Al. For a polycrystalline Al sample subject to the deformation with $u_{xx} = 0.03$, the CPD amounts to $-0.025 \pm 0.002 \text{ V}$ [5]. Because a polycrystalline sample can be considered as being assembled from arbitrarily oriented single crystals, the values obtained by us must be averaged in order to compare them with experiment. Thus, both the experiment and the calculations give a negative change of the surface potential,

$$\text{CPD} = \Delta v_{\text{eff}}(z = z_0) < 0.$$

For the conventional method of measuring the work function changes upon strain [4, 5, 9], this implies that

$$W(u_{xx}) = W(0) - \text{CPD}(u_{xx}) > W(0),$$

i.e., the work function increases for a tensed sample. In general, therefore, our results agree with the independent experiments for both stretched [4–6] and compressed [1, 3] metal samples. The results for $\Delta v_{\text{eff}}(u_{xx})$ correspond to a direct observation of the stress-induced shift in the measured contact potential: the effective potential outside the open faces of the sample is more negative/positive when tensile/compressive force is applied. However, unlike the effective potential at the surface, the value of the potential in the metal bulk is more positive/negative for an expanded/compressed sample because of the different effect of the $\langle \delta v \rangle_{\text{face}}$ term. Thus, for the Al sample, the work function change vs. strain shows the opposite trend compared to that of the contact potential (the behavior of which also differs from that predicted by non self-consistent calculations [27]). Accordingly, the results in Table 1 demonstrate that the work function decreases with u_{xx} . In other words, our results show that the measurements by the Kelvin method give not the variation of the work function upon strain but the variation of the surface potential.

In summary, the stabilized-jellium model has been extended to encompass the elastic strain effects on surface properties of simple metals. By imposing a uniaxial strain to the metal surface and limiting ourselves to linear terms in the deformation, we have obtained a realistic description of the strain dependence of surface quantities: surface energy, surface stress, and work function. We have presented a consistent explanation of

experiments on the stress-induced contact potential difference at metal surfaces.

The authors are grateful to A. Kiejna for his help in numerical calculations. One of the authors (V. V. P.) would like to thank the Institute of Experimental Physics at the University of Wrocław for kind hospitality. This work was partly supported by the NATO "Science for Peace" Program (project SFP-974109).

REFERENCES

1. F. C. Witteborn and W. N. Fairbank, *Phys. Rev. Lett.* **19**, 1049 (1967).
2. Sh. M. Kogan, *Usp. Fiz. Nauk* **105**, 157 (1971) [*Sov. Phys. Usp.* **14**, 658 (1972)].
3. P. P. Craig, *Phys. Rev. Lett.* **22**, 700 (1969).
4. P. I. Mints, V. P. Melekhin, and M. B. Partensky, *Fiz. Tverd. Tela (Leningrad)* **16**, 3584 (1974) [*Sov. Phys. Solid State* **16**, 2330 (1974)].
5. S. V. Loskutov, *Fiz. Met. Metalloved.* **86**, 149 (1998).
6. J. W. Beams, *Phys. Rev. Lett.* **21**, 1093 (1969).
7. W. A. Harrison, *Phys. Rev.* **180**, 1606 (1969).
8. Yu. A. Kulyupin and S. A. Nepijko, *Fiz. Tverd. Tela (Leningrad)* **17**, 2747 (1975) [*Sov. Phys. Solid State* **17**, 1822 (1975)].
9. V. V. Levitin, S. V. Loskutov, M. I. Pravda, and B. A. Serpetzky, *Solid State Commun.* **92**, 973 (1994).
10. A. Kiejna and K. F. Wojciechowski, *Metal Surface Electron Physics* (Pergamon, Oxford, 1996).
11. E. L. Nagaev, *Usp. Fiz. Nauk* **162** (9), 49 (1992) [*Sov. Phys. Usp.* **35**, 747 (1992)].
12. A. Ya. Gohshtein, *Usp. Khim.* **44**, 1956 (1975).
13. A. Kiejna and P. Ziesche, *Solid State Commun.* **88**, 143 (1993).
14. J. P. Perdew, *Prog. Surf. Sci.* **48**, 245 (1995).
15. P. J. Feibelman, *Phys. Rev. B* **50**, 1908 (1994).
16. H. L. Skriver and N. M. Rosengaard, *Phys. Rev. B* **46**, 7157 (1992).
17. J. P. Perdew, Y. Wang, and E. Engel, *Phys. Rev. Lett.* **66**, 508 (1991).
18. V. V. Pogosov, *Solid State Commun.* **89**, 1017 (1994).
19. R. Shuttleworth, *Proc. Phys. Soc. London, Sect. A* **63**, 444 (1950).
20. R. C. Cammarata, *Prog. Surf. Sci.* **46**, 1 (1994).
21. P. Ziesche, J. P. Perdew, and C. Fiolhais, *Phys. Rev. B* **49**, 7916 (1994).
22. P. Ziesche, in *Density Functional Theory*, Ed. by E. K. U. Gross and R. M. Dreizler (Plenum, New York, 1995), p. 559.
23. I. Langmuir, *Chem. Rev.* **13**, 147 (1933).
24. W. A. Tiller, S. Ciraci, and I. P. Batra, *Surf. Sci.* **65**, 173 (1977).
25. J. P. Perdew, H. Q. Tran, and E. D. Smith, *Phys. Rev. B* **42**, 11627 (1990).
26. A. Kiejna, *Prog. Surf. Sci.* **61**, 85 (1999).
27. V. V. Pogosov, *Solid State Commun.* **81**, 129 (1992).
28. R. Smoluchowski, *Phys. Rev.* **60**, 661 (1941).
29. N. D. Lang and W. Kohn, *Phys. Rev. B* **3**, 1215 (1971).
30. I. I. Tupizin and I. V. Abarenkov, *Phys. Status Solidi B* **82**, 99 (1977).
31. N. W. Ashcroft and N. D. Mermin, *Solid State Physics* (Holt, Rinehart and Winston, New York, 1976).
32. A. Kiejna and P. Ziesche, *Phys. Rev. B* **56**, 1095 (1997).
33. A. K. Theophilou and A. Modinos, *Phys. Rev. B* **6**, 81 (1972).
34. A. Kiejna and V. V. Pogosov, *J. Phys.: Condens. Matter* **8**, 4245 (1996).
35. J. M. Kras, J. M. van Ruitenbeek, V. V. Fisun, *et al.*, *Nature* **375**, 767 (1995).
36. G. Rubio, N. Agrait, and S. Viera, *Phys. Rev. Lett.* **76**, 2302 (1996).
37. E. G. Brovman and Yu. Kagan, *Usp. Fiz. Nauk* **112**, 369 (1974) [*Sov. Phys. Usp.* **17**, 125 (1974)].
38. L. D. Landau and E. M. Lifshitz, *The Classical Theory of Fields* (Nauka, Moscow, 1973; Pergamon, Oxford, 1975).
39. L. V. Tikhonov, V. A. Kononenko, G. I. Prokopenko, and V. A. Rafalovsky, *Structure and Properties of Metals and Alloys* (Naukova Dumka, Kiev, 1986).
40. R. G. Linford, L. A. Mitchel, C. Osgood, and M. P. Williams, *Surf. Sci.* **219**, 341 (1989).
41. R. J. Needs and M. J. Godfrey, *Phys. Rev. B* **42**, 10933 (1990).

SPELL: Zaporozhye, jellium, aluminium, positrons, estans, crystallite, standart, explaining, nanowires, polycrystal, uniaxially, prolate